

ON VISION-BASED KINEMATIC CALIBRATION OF n -LEG PARALLEL MECHANISMS

P. Renaud¹, N. Andreff¹, G. Gogu¹, P. Martinet²

¹ *Laboratoire de Recherches et Applications en Mécanique Avancée
IFMA – Université Blaise Pascal, 63175 Aubière, France*

² *Laboratoire des Sciences et Matériaux pour l'Electronique et d'Automatique
Université Blaise Pascal – CNRS, 63175 Aubière, France*

Abstract: A vision-based kinematic calibration algorithm is proposed for parallel mechanisms with end-effector connected to the base by n legs. The joint between corresponding leg ends can be a passive or actuated prismatic joint, which include constant-length legs. Information on the position and orientation of the mechanism legs is extracted from the observation of these elements with a standard camera. No workspace limitation nor installation of additional proprioceptive sensors are required. The algorithm is first detailed, then an evaluation of the method is achieved for a Stewart-Gough platform, with experimental measurement accuracy evaluation and simulation of the identification process. *Copyright © 2002 IFAC*

Keywords: robotics, parameter identification, physical parameters, nonlinear equations, computer vision.

1. INTRODUCTION

Compared to serial mechanisms, parallel structures exhibit a much better repeatability (Merlet, 1997), but not better accuracy (Wang and Masory, 1993). A kinematic calibration is thus also needed. Among the algorithms proposed to conduct calibration for these structures, methods based on the use of additional proprioceptive sensors on the passive joints are interesting, because they enable one to have a unique solution to the direct kinematic model (Tancredi, 1995), and then to use a criterion based on this model. An alternate way is to use the additional sensors on some legs to express a direct or inverse kinematic model as a function of the parameters of these legs and the redundant information. Calibration can then be achieved in a single process (Wampler and Arai, 1992, Zhuang, 1997) or in two steps (Daney, 2000). The main advantages of these methods are then the absence of workspace limitation and the analytical expression of the identification criterion. However, practically speaking, the design

of the mechanism has to take into account the use of these sensors. Furthermore, for some mechanisms, the passive joints can not be equipped with additional sensors, for instance spherical joints. Consequently, the proposed method combines the advantage of information redundancy on the legs with non-contact measurements to perform the kinematic calibration.

The parallel mechanisms are designed with slim, often cylindrical, legs that link the end-effector and the base. The kinematic behavior of the mechanism is closely related to the movement of these legs. Hence the study of their geometry has already led to singularity analysis based on line geometry (Merlet, 1988). For such geometrical entities, the image obtained with a camera can be bound to their position and orientation with respect to the camera. By observing simultaneously several legs, it is then possible to get information on their relative position. Calibration can be achieved by deriving an identification algorithm adapted to this information. No workspace limitation is introduced, nor modification of the mechanism.

In this article, an algorithm is introduced for vision-based kinematic calibration of parallel mechanisms by observation of the mechanism legs. The method is developed in the context of mechanisms with n legs. The joints between corresponding leg ends can be passive or actuated prismatic joints, which include constant-length legs, and joints at leg ends may be revolute, spherical or universal joints. The method is composed of four steps: the first one consists of determining in the camera frame the parameters of the joints linked to the base. The second step enables one to estimate these parameters in the base frame, then in a third step the actuator encoder offsets are identified. Finally, in the fourth step, the parameters of the joints between the legs and the end-effector are identified.

The second section presents the mechanism modelling. The identification algorithm is then detailed in the third section, recalling first the relation between position and orientation of a cylindrical axis and its image projection. The four steps of the identification process are then detailed. In the fourth section, an evaluation of the proposed method is achieved by an experimental estimation of the measurement accuracy and a simulation of the identification of a Deltalab Stewart-Gough platform. Conclusions are then finally given on the performance and further developments of this method.

2. KINEMATIC MODELLING

The mechanism to identify is a parallel structure with n legs between the base and the end-effector (Fig. 1). The joint between corresponding leg ends can be a passive or actuated prismatic joint, which include constant-length legs. The desired end-effector pose is achieved by modifying the actuated leg lengths. The legs are considered connected to the base with revolute (R), spherical (S) or universal (U) joints. Many mechanisms have such a structure: 3-(RPR), 3-(UPU) (Fig. 1), 6-(SPU), ... According to the analysis achieved for the Stewart-Gough platform (Wang and Masory, 1993), these joints are supposed to be perfect. A revolute joint is then defined by its joint center and its axis direction. A universal joint is composed of two consecutive perpendicular revolute joints having a common intersection point. This joint is therefore defined by its joint center and the direction of the first rotation axis, linked either to the base or to the end-effector. Eventually, a spherical joint is defined by its joint center.

For manipulators, the controlled pose is the Euclidean rigid transformation between the world frame R_w and the tool frame R_t (Fig. 1). Noting R_b the frame defined by the joints between the legs and the base and R_e the frame defined by the joints between effector and legs, two transformations wT_b and eT_t can be defined between world and base frames and between end-effector and tool frames. These transformations are however dependent on the

application and must be identified for each tool and relocation of the mechanism. Therefore the only considered kinematic parameters define relatively the joint parameters on the base and the end-effector, and the actuator encoder offsets. The transformations wT_b and eT_t can be identified by other techniques (Tsai and Lenz, 1989, Andreff *et al.*, 2001).

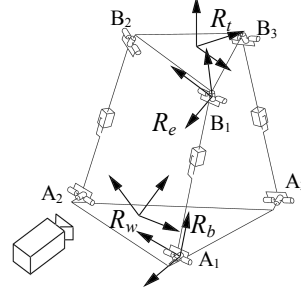


Fig. 1. Example of identifiable mechanism: 3-(UPU) parallel mechanism and the camera.

3. ALGORITHM

3.1 Vision-based Information Extraction

Projection of a cylinder In this paragraph, the relationship between the position and orientation of the legs of the mechanism, supposed to be cylindrical of known radius R , and their image is expressed. The image formation is represented by the pinhole model (Faugeras, 1993) and the camera is assumed to be calibrated. In such a context, a cylinder image is composed of two lines (Fig. 2), generally intersecting except if the cylinder axis is going through the center of projection. Each corresponding generating line D_i , $i \in [1,2]$ can be defined in the camera frame $R_c(C, x_c, y_c, z_c)$ by its Plücker coordinates (Pottmann *et al.*, 1998) $(\underline{u}_i, \underline{h}_i)$ with \underline{u}_i the unit axis direction vector and \underline{h}_i defined by:

$$\underline{h}_i = \underline{u}_i \times \underline{CP} \quad (1)$$

where \underline{P} is an arbitrary point of D_i , and \times represents the vector cross product.

Each generating line image d_i can be defined by a triplet (a_i, b_i, c_i) such that this line is defined in the sensor frame $R_s(O, x_s, y_s)$ by the relationship:

$$\begin{cases} (a_i & b_i & c_i)(x & y & 1)^T = 0 \\ a_i^2 + b_i^2 + c_i^2 = 1 \end{cases} \quad (2)$$

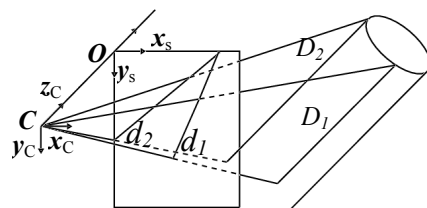


Fig. 2. Perspective projection of a cylinder and its outline in the sensor frame.

Due to perspective geometry, (a_i, b_i, c_i) and \mathbf{h}_i are colinear. Provided that lines are oriented, one has:

$$(a_i, b_i, c_i)^T = \frac{\mathbf{h}_i}{\|\mathbf{h}_i\|} = \underline{\mathbf{h}}_i \quad (3)$$

Determining the cylinder axis direction from the image Since the projection $(\underline{\mathbf{h}}_1, \underline{\mathbf{h}}_2)$ of the cylinder is now known, the cylinder axis direction $\underline{\mathbf{u}}$ can be computed by:

$$\underline{\mathbf{u}} = \frac{\underline{\mathbf{h}}_1 \times \underline{\mathbf{h}}_2}{\|\underline{\mathbf{h}}_1 \times \underline{\mathbf{h}}_2\|} \quad (4)$$

Determining the cylinder axis position from the image Furthermore the distances between the cylinder axis and the generating lines are equal to the cylinder radius. Let $\mathbf{M}(x_M, y_M, z_M)$ be a point of the cylinder axis. As $\underline{\mathbf{h}}_i$ is computed as a unit vector, the belonging of \mathbf{M} to the axis can be expressed by the two equations:

$$\underline{\mathbf{h}}_i^T \mathbf{M} = \varepsilon_i R, i \in [1, 2] \quad (5)$$

with $\varepsilon_1 = \pm 1$, $\varepsilon_2 = -\varepsilon_1$. The determination of ε_1 is performed in the grayscale image by analyzing the position of the cylinder with respect to the generating line d_1 . As the lines are chosen with the same orientation, ε_1 and ε_2 are of opposite sign.

It can be easily proved that the kernel dimension of $[\underline{\mathbf{h}}_1 \ \underline{\mathbf{h}}_2]^T$ is equal to one, by decomposing \mathbf{M} on the orthogonal basis $(\underline{\mathbf{u}}, \underline{\mathbf{h}}_1, \underline{\mathbf{u}} \times \underline{\mathbf{h}}_1)$. The system (5) is therefore under-determined. The position of \mathbf{M} can be computed in several ways, for instance by choosing a particular point as $\mathbf{M}_{LS}(x_{MLS}, 0, z_{MLS})$, under condition of its existence.

From the observation of one leg with a camera, it is thus possible to determine the position and orientation of its axis in the camera frame.

3.2 Joint Parameters Estimation in the Camera Frame

In this section, the relationships necessary to determine the joint parameters in the camera frame are derived. For each joint j , N_I images of the corresponding leg are stored for different end-effector poses, which enables one to compute in the camera frame the leg axis orientation $\underline{\mathbf{u}}_{j,k}$ and the leg axis point $\mathbf{M}_{j,k}$, $k \in [1, N_I]$.

Joint Center For spherical, universal and revolute joints, the position of the joint center \mathbf{A}_j in R_c can be computed by expressing its belonging to the axis for the N_I poses:

$$\mathbf{A}_j \mathbf{M}_{j,k} \times \underline{\mathbf{u}}_{j,k} = \mathbf{0}, k \in [1, N_I] \quad (6)$$

The joint center \mathbf{A}_j is determined by solving the over-determined system obtained by concatenation of the $3T$ equations expressed in (6). As the three equations provided by the cross product are not independent, the solution is obtained by singular value decomposition. At least two different axis orientations are necessary to estimate the joint center.

Joint axis For a revolute joint, the joint axis $\underline{\mathbf{v}}_j$ is perpendicular to the leg axis orientation vectors $\underline{\mathbf{u}}_{j,k}$:

$$\underline{\mathbf{v}}_j \cdot \underline{\mathbf{u}}_{j,k} = 0, k \in [1, N_I] \quad (7)$$

The joint axis $\underline{\mathbf{v}}_j$ can be determined by solving the over-determined system obtained by concatenation of the N_I equations expressed in (7). At least two different leg orientations are necessary to estimate the parameters.

For a universal joint, if the first joint axis direction has an influence on the mechanism kinematics, its orientation will be computed in the fourth step (3.5).

3.3 Joint Parameters Estimation in the Base Frame

Identification criterion Because of leg visibility conditions, it may be necessary to move the camera around the mechanism. N_C different camera positions are therefore considered. The end-effector poses are not supposed to be identical for each camera position.

The base frame is defined using N_d joint centers ($N_d=2$ for a planar mechanism, $N_d=3$ for a spatial mechanism).

For a camera position defined by the camera frame R_{ca} , n_α legs can be observed for any end-effector pose, which include r_α legs with revolute joints on the base. Let N_α the whole observable leg set, and R_α the set of observable legs connected to the base with revolute joints. The joint parameters have been computed in R_{ca} using (6-7). From the n_α joint centers on the base, $(n_\alpha - 1)$ independent vectors $\mathbf{A}_j \mathbf{A}_g$, $(j, g) \in N_\alpha$ can be computed.

Let \mathbf{V} be the union of this vector set and the revolute joint axes:

$$\mathbf{V} = \{\mathbf{A}_j \mathbf{A}_g, (j, g) \in N_\alpha\} \cup \{\underline{\mathbf{v}}_j, j \in R_\alpha\} \quad (8)$$

With its elements, $C_{r_\alpha}^2 + C_{n_\alpha}^2 + r_\alpha(n_\alpha - 1)$ independent scalar products can be computed. Using the scalar product invariance with frame transformation, the joint parameters in the base frame are computed by non-linear minimization of the criterion C_I :

$$C_I = \sum_{\alpha=1}^{N_C} \sum_{p,q} \left[\mathbf{V}_p \cdot \mathbf{V}_q \Big|_{R_{ca}} - \mathbf{V}_p \cdot \mathbf{V}_q \Big|_{R_b} \right]^2 \quad (9)$$

with N_C the number of camera positions, \mathbf{V}_j the j -th

element of V and $\cdot|_R$ denoting the reference frame (R) in which the vectors V_j are expressed.

Identifiability conditions To perform joint parameters determination in the base frame, two conditions have to be fulfilled: Firstly, all the legs have to be observed at least once. Secondly, the number of equations has to be greater or equal to the number of parameters to identify. For a planar mechanism, two joint centers define the base frame, and one parameter defines the plane perpendicular. The number N_p of parameters to identify is hence equal to:

$$N_p = 2 + 2(n - N_d) \quad (10)$$

In the same way, for a spatial mechanism:

$$N_p = 3 + 3(n - N_d) + 2r \quad (11)$$

with r the total number of revolute joints. The second identifiability condition is then:

$$\sum_{\alpha=1}^{N_C} (C_{r_\alpha}^2 + C_{n_\alpha}^2 + r_\alpha(n_\alpha - 1)) \geq N_p \quad (12)$$

At the end of this second step, the joint parameters in the base frame are determined, without any other assumption on the kinematics than the absence of joint clearance.

If the previously outlined identifiability conditions can not be fulfilled, the use of an additive calibration board linked to the base enables one to compute for each leg its position and orientation *w.r.t* the camera frame and, simultaneously, the pose of the camera *w.r.t* the calibration board (Dhome *et al.*, 1989). The gathering of the data for the different camera positions is then possible.

3.4 Actuator Encoder Offsets Estimation

Identification criterion In this third step, the actuator encoder offsets and the constant leg lengths are identified. For each successive camera frame $R_{c\alpha}$, the joint center positions A_j on the base and the axis orientations $\underline{u}_{j,k}$ are known. The position of the leg end $B_{j,k}$ can therefore be computed for the N_l poses as a function of only the offsets q_{0j} in the camera frame:

$$B_{j,k}|_{R_{c\alpha}} = A_{j,R_{c\alpha}} + (q_{j,k} + q_{0j})\underline{u}_{j,k}|_{R_{c\alpha}}, k \in [1, N_l] \quad (13)$$

Let n_{AC} the number of legs with actuated prismatic joints or constant-length legs, and AC_α the set of n_{AC_α} such legs observed for the camera position α .

A number $C_{n_{AC_\alpha}}^2$ of distances $\|B_j B_g\|$ can be expressed and, by comparing the value of these distances between two consecutive positions, an error

function C_2 can then be expressed as a function of the n_{AC} offsets $q_{0j}, j \in [1, n_{AC}]$:

$$C_2 = \sum_{\alpha=1}^{N_C} \sum_{k=1}^{N_l-1} \sum_{\substack{(j,g) \in AC_\alpha \\ g > j}} \left[\|B_{j,k+1} B_{g,k+1}\|_{R_{c\alpha}} - \|B_{j,k} B_{g,k}\|_{R_{c\alpha}} \right]^2 \quad (14)$$

with $B_{j,k}$ the position of B_j for the k -th end-effector pose. The offsets are obtained by nonlinear optimization of C_2 .

Notice that this includes the case of constant-length legs, where the actuator encoder value is equal to zero in the criterion C_2 and the joint offset is equal to the leg length.

Identifiability conditions The offsets identification can only be achieved if each leg can be observed with the camera for at least one camera position, which is already necessary in the previous step. The number of relationships has also to be greater or equal to the number n_{AC} of joint offsets:

$$\sum_{\alpha=1}^{N_C} (C_{n_{AC_\alpha}}^2) \geq n_{AC} \quad (15)$$

3.5 Joint Parameters Estimation in the End-Effector Frame

Joint centers The determination of the joint offsets enables one to compute the average value of $\|B_j B_g\|$ for n_{AC} legs and therefore the relative position of the joints on the end-effector. Using the distance invariance with frame transformation the joint center positions in the end-effector frame can be identified by non-linear minimization of the criterion C_3 :

$$C_3 = \sum_{\alpha=1}^{N_C} \sum_{(j,g) \in AC_\alpha, g > j} \left[\|B_j B_g\|_{R_{c\alpha}} - \|B_j B_g\|_{R_e} \right]^2 \quad (16)$$

To perform this joint center determination, two conditions have to be fulfilled. Each leg has to be observed for at least one camera position. Furthermore, the number of equations has to be greater or equal to the number E of parameters, with $E = l + 2(n - N_d)$ for a planar mechanism, and $E = 3 + 3(n - N_d)$ for a spatial mechanism:

$$\sum_{\alpha=1}^{N_C} C_{n_{AC_\alpha}}^2 \geq E \quad (17)$$

Revolute joint axes The transformation between the camera frame and the end-effector frame ${}^{R_C}T_{R_e} = ({}^{R_C}R_{R_e}, {}^{R_C}t_{R_e})$ can be computed from the positions $B_{j,k}$ in these frames ($j \in N_{R_\alpha}, k \in [1, N_l]$):

$$\left({}^{R_C}R_{R_e} B_{j,k}|_{R_e} + {}^{R_C}t_{R_e} \right) \times B_{j,k}|_{R_C} = \mathbf{0} \quad (18)$$

The computation is achieved by solving the nonlinear system obtained by concatenation of the equation (18) for the observable leg set N_{R_α} . Three legs, including the one with a revolute joint on the end-effector, need to be observed for one camera position: $N_{R_\alpha} \geq 3$.

This enables one to express the leg axis orientation $\underline{u}_{j,k}$ and the axis point \mathbf{M}_k in the end-effector frame for each position k . The determination of the joint axis is then similar to the determination achieved in the second step (3.2). For a planar mechanism, the joint axis directions are already identified on the base.

Universal joint axes The computation of the transformation between camera and base frame ${}^{R_C}T_{R_b}$ is similar to the estimation of ${}^{R_C}T_{R_e}$ in the previous paragraph. Three legs have to be observed simultaneously. If so, the transformation between base and end-effector frames ${}^{R_b}T_{R_e}$ can then be estimated, and the use of the inverse kinematic model enables one to identify the universal joint axes.

Passive legs From the knowledge of ${}^{R_C}T_{R_e}$ solving equation (18), the position of a passive leg end on the end-effector can be expressed in the camera frame as a function of this transformation and its position in the end-effector frame. Three actuated legs need to be observed simultaneously. The belonging of the passive leg end to the axis can then be expressed by:

$$\underline{u}_{j,k}|_{R_C} \times \mathbf{A}_j \mathbf{B}_j|_{R_C} = \mathbf{0}, k \in [1, N_I] \quad (19)$$

The joint center is computed by solving the over-determined linear system obtained by concatenation of the equation (19). At least two different axis orientations are necessary.

4. METHOD EVALUATION

The proposed method is evaluated for the Deltalab Stewart-Gough platform (Fig. 3) as follows: First the calibration conditions are detailed. Then the measurement accuracy is experimentally evaluated, and the simulation of the identification process with the formerly evaluated measurement noise is achieved. To estimate the calibration method performance, analysis of the identified parameters and accuracy improvement is eventually conducted.

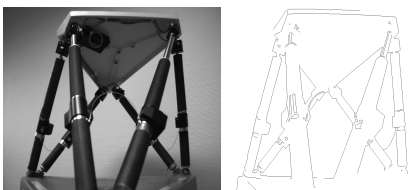


Fig. 3: The Stewart-Gough platform (left) and its image after edge detection (right).

4.1 Calibration Conditions

The structure is a 6-(SPU) parallel mechanism. The kinematic model is however not sensitive to the joint axis direction of the U-joints. Consequently, the only identified parameters are the joint locations on the base and the end-effector and the six actuator offsets: $n=6$, $N_d=3$. Because of the symmetry of the mechanism (Fig. 3), three different camera positions are considered (*i.e.* $N_C=3$). From (12), the simultaneous observation of four legs is then sufficient: $n_a=4$.

4.2 Measurement Accuracy

Six equally-spaced leg orientations are considered within the extremal values. The measurement accuracy is evaluated from a set of consecutive measurements, for each leg position.

A 1024×768 camera with a 6mm lens is used to acquire the images, connected to a PC via an IEEE1394 bus. Cylinder outline detection is achieved by means of a Canny filter (Canny, 1986) (Fig. 3). Lines are then computed from the detected points by a least-squares method.

In Table 1, the upper-bound of the estimated standard deviations of the cylinder position and orientation are listed. The orientation is described with the Euler angles (ψ, θ) . The position is obtained by estimating the point $\mathbf{M}_{LS}(x_{MLS}, 0, z_{MLS})$.

Table 1 Upper-bound of the standard deviations

Parameter	ψ	θ	x_{MLS}	z_{MLS}
Est. st. dev.	0.05rad	0.06rad	0.05mm	0.1mm

It must be stated that the image processing could be improved by the use of a subpixel detection filter (Steger, 1997) and now available higher CCD resolution sensor, since the accuracy is intrinsically bound to this resolution.

4.3 Simulation

Performance Evaluation Simulation allows one to evaluate directly the knowledge improvement of the kinematic parameter values. Let ξ_{gt_i} be the ground-truth value of the i -th kinematic parameter ($i \in [1, 30]$), and ξ_{id_i} its identified value. The calibration gain can then be computed by the estimation error $|\xi_{id_i} - \xi_{gt_i}|$.

In order to evaluate the influence of a parameter estimation error, the displacement error ΔX and the orientation error ΔE are computed for ten randomly chosen poses:

$$\begin{cases} \Delta X = \|\mathbf{A}_I \mathbf{B}_I \xi_{gt} - \mathbf{A}_I \mathbf{B}_I \xi_{id}\| \\ \Delta E = \|\Delta \psi \quad \Delta \theta \quad \Delta \phi\| \end{cases} \quad (20)$$

where $(\Delta \psi, \Delta \theta, \Delta \phi)$ are the Euler angles defining the

difference between the end-effector orientation computed with the kinematic parameter sets ξ_{gt} and the one computed with ξ_{id} .

Simulation Process Fifteen end-effector poses are generated by randomly selecting configurations with extreme leg lengths. These leg lengths are corrupted with noise to simulate proprioceptive sensor measurements (uniformly distributed noise, variance equal to $3\mu m$). The leg orientation and axis points M_i are modified by addition of white noise with standard deviation equal to those previously estimated in Table 1. For each end-effector pose, three images are acquired with the camera to reduce the measurement noise. Initial kinematic parameter values are obtained by addition to the model values of a uniform noise with variance equal to 2mm. The base and end-effector frames are defined using joint centers 1, 3 and 5.

Results Figure 4 represents the ground-truth parameter values and the mean estimation errors $Mean|\xi_{id_i} - \xi_{gt_i}|$, computed by 100 simulations of the calibration. A sharp improvement of the knowledge of the kinematic parameters is observed, except for the z component of the joint locations. The parameter estimation errors are however low with an average error between 0.04mm and 1mm.

It must also be underlined that the accuracy improvement is significant with an average displacement error reduced from 1mm for the initial kinematic parameters to 0.08mm, and an orientation error reduced from 0.12rad to 0.018rad.

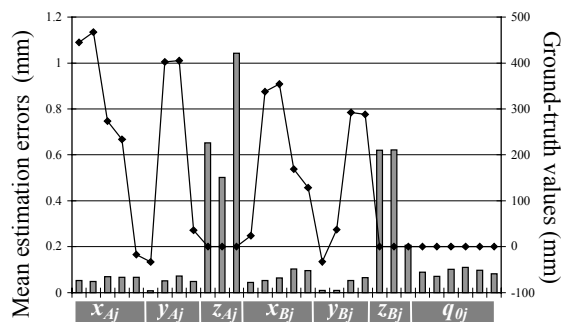


Fig. 4: Mean estimation errors (bars) and ground-truth values (line) of the thirty parameters.

5. CONCLUSION

In this article, a vision-based calibration method for mechanisms with n legs between the base and the end-effector has been proposed. Using an exteroceptive sensor, the kinematic parameters of the structure are identified. No mechanical constraint nor additional proprioceptive sensor are required. The method is low-cost as standard off-the-shelf cameras are used. The identification criteria and identifiability conditions have been derived. The experimental evaluation of the measurement accuracy and the

simulation results show a significant accuracy improvement for a Deltalab Stewart-Gough platform. The algorithm performance can be improved by using more accurate detection algorithms, and a better selection of the end-effector poses for calibration, which will soon be implemented. The method will be also validated for other mechanisms.

ACKNOWLEDGEMENT

This study was jointly funded by CPER Auvergne 2001-2003 and by the CNRS-ROBEA program through the MAX project.

REFERENCES

- Andreff N., Horaud R. and Espiau B. (2001). Robot hand-eye calibration using structure-from-motion, *Int. J. Rob. Research*, **20**(3), pp. 228-248.
- Canny J.F. (1986). A computational approach to edge detection, *IEEE Trans. Pattern Analysis and Machine Intelligence*, **8**(6), pp.679-698.
- Daney D. (2000). Etalonnage géométrique des robots parallèles. PhD Thesis, Université de Nice.
- Dhome M., Richetin M., Lapreste J.T. and Rives G. (1989). Determination of the Attitude of 3-D Objects From A Single Perspective View, *IEEE Trans on Pattern Analysis and Machine Intelligence*, **11**(12), pp.1265-1278.
- Faugeras O. (1993). *Three-dimensional Computer Vision: A Geometric Viewpoint*, The MIT Press.
- Merlet J.P. (1988). Parallel manipulators, Part 2, Singular Configurations and Grassmann geometry, *Res. Report RR-0791T*, INRIA.
- Merlet J.P. (1997). *Les Robots Parallèles*, Hermès.
- Pottmann H., Peternell M. and Ravani B. (1998). Approximation in line space – applications in robot kinematics and surface reconstruction, In: *Advances in Robot Kinematics: Analysis and Control*, pp. 403-412, Strobl.
- Steger C. (1997). Removing the Bias from Line Detection, In: *Computer Vision and Pattern Recognition '97*, pp. 116-122, Puerto Rico.
- Tancredi L. (1995). De la simplification et la résolution du modèle géométrique direct des robots parallèles, PhD Thesis, Ecoles des Mines de Paris.
- Tsai R.Y. and Lenz R.K. (1989). A new technique for fully autonomous and efficient 3D robotics hand/eye calibration. *IEEE Trans. On Rob. and Automation*, **5**(3), pp. 345-358.
- Wampler C. and Arai T. (1992). Calibration of Robots Having Kinematic Closed Loops Using Non-Linear Least-Squares Estimation, In: *Proc. IFToMM-jc Int. Symp. On Theory of Machine and Mechanisms*, pp.153-158, Nagoya.
- Wang J. and Masory O. (1993). On the Accuracy of a Stewart Platform – Part I: The Effect of Manufacturing Tolerances, In: *Proc. of ICRA*, pp.114-120, Atlanta.
- Zhuang H. (1997). Self Calibration of Parallel Mechanisms With a Case Study on Stewart Platforms, *IEEE Trans. On Robotics and Automation*, **13**(3):387-397.